

High-resolution Displacement Sensor with Ultrahigh Compactness Based on Self-imaging Effect of Optical Microgratings

line 1: Mengdi Zhang
line 2: School of Instrument and Electronics
line 3: North University of China
line 4: Taiyuan, China
line 5: zmd991111@163.com

line 1:Chenguang Xin
line 2: School of Instrument and Electronics
line 3: North University of China
line 4: Taiyuan, China
line 5: xincg@nuc.edu.cn

Abstract—Based on self-imaging effect of 3μm-period microgratings, a novel displacement sensor is demonstrated. With no using optical components such as reflectors, polarizers and splitters, the sensor shows ultrahigh compactness with a resolution down to ~0.7nm.

Keywords—optical micrograting, self-imaging, displacement, sensor

High-resolution displacement measurement sensors have been used in different applications such as mechanical processing and semiconductor manufacturing[1]. Traditional high-resolution displacement measurement technologies include capacitive displacement sensing technology[2], laser interferometric displacement sensing technology[3], grating displacement sensing technology[4], etc. Benefitting from a high resolution, a compact structure and a good stability, the grating-based approach is typically used in machines such as lithography machines and machine tools[5]. Such sensors are generally based on interference between different diffracted beams of an optical micrograting. As a result, a complicated system consisting of reflectors, polarizers, splitters and wave plates are required. Considering the recent interesting in developing miniaturized positioning systems, displacement sensors with high resolution and ultra-compact structure is still in high demand. Here we propose an ultra-compact displacement sensor with resolution down to ~0.7 nm. Based on self-imaging effect of 3μm-period microgratings, sinusoidal signals are obtained by detecting the transmitted amplitude of a double-grating structure. Using a interpolation circuit with subdividing factor of 4096, a sub-nanometer resolution of ~0.7 nm is demonstrated experimentally. In addition, measurement of vibration with frequency of 70Hz has also been carried out in experiment, indicating the ability for the proposed sensor for vibration measurement. Without using much optical components such as reflectors and polarizers, the sensor has an ultra-compact structure, which show great potential in applications such as miniaturized positioning systems.

I. Principle

Self-imaging effect refering to the periodic intensity patterns containing the replication of grating patterns with different distances can be observed in the triangle area (Talbot area) behind the grating under the illumination of parallel coherent beams, the distances between the self-imaging patterns along the optical axis can be given by [6]:

$$Z_T = N \frac{2d^2}{\lambda} (n = 1, 2, 3, \dots) \quad (1)$$

where d is the grating period, λ is the light source wavelength.

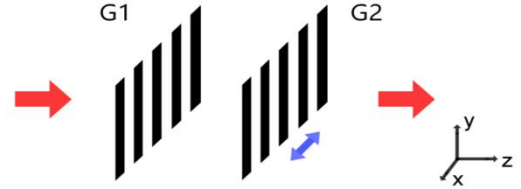


Fig.1. Schematic diagram of a double-layer grating structure.

The measuring principle of the proposed sensor can be explained by a plane wave interference theory[7]. As shown in Figure 1, a double-layer structure consisting of two optical microgratings with a same period is proposed. When a monochromatic plane wave is vertically incident on an optical grating (G1), the complex amplitude distribution of the light wave transmitted from the grating can be expressed as

$$u(x_0) = t(x_0) = \sum_{n=-\infty}^{\infty} C_n \exp\left(i2\pi \frac{n}{d} x_0\right) \quad (2)$$

where C_n is the Fourier coefficient, $t(x_0)$ is the radiation transmission function of a single grating. The complex amplitude transmittance function of the lower grating can be expressed as

$$t'(x_0) = \sum_{m=-\infty}^{\infty} C_m \exp\left(i2\pi \frac{m}{d} x_0\right) \quad (3)$$

Assuming that the second grating (G2) is placed behind G1 with a distance of z , the complex amplitude distribution of the plane light field behind G2 can be expressed as

$$U'(x) = \sum_{n=-\infty}^{\infty} \sum_{m=-\infty}^{\infty} C_n C_m \exp\left\{i2\pi \frac{n+m}{d} x\right\} \exp\{i2\pi n \Delta x / d\} \exp\{i2\pi n z / \lambda\} \exp\{-i2\pi n^2 z \lambda / d^2\} \quad (4)$$

where Δx is the relative displacement between the double-layer gratings.

The intensity distribution behind G2 after Fourier transform can be given as[8]

$$I(x) = \sum_{n=-\infty}^{\infty} \sum_{m=-\infty}^{\infty} \sum_{p=-\infty}^{\infty} \sum_{q=-\infty}^{\infty} C_n C_m C_p C_q \exp\left\{i2\pi \frac{(n-p)+(m-q)}{d} x\right\} \exp\{-i2\pi(p-n)\Delta x / d\} \exp\{-i2\pi(p^2 - n^2)z \lambda / d^2\} \quad (5)$$

II. Simulation analysis

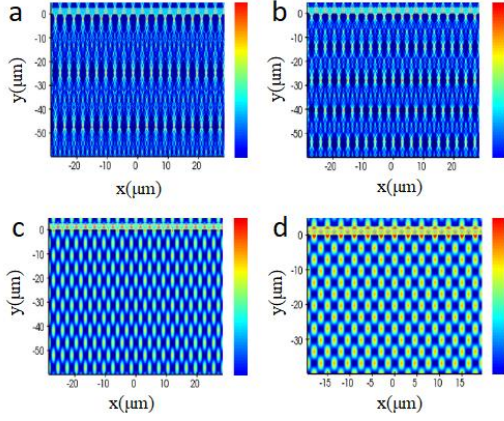


Fig.1. Simulated self-imaging patterns with a 3 μm -period micrograting. The wavelength of input light is (a)375nm, (b)635nm, (c)1.5 μm and (d) 2.2 μm , respectively .

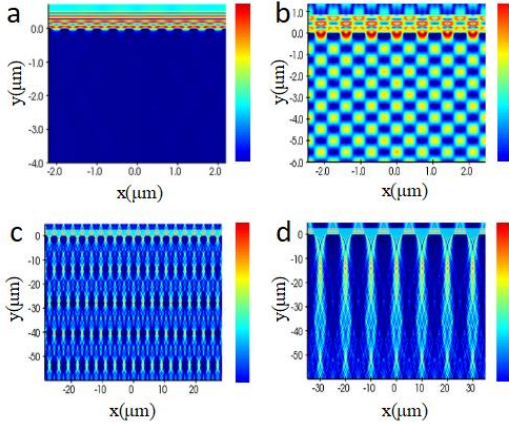


Fig.2. Simulated self-imaging patterns with wavelength of 635nm. The periods of microgratings are (a)400nm, (b)700nm, (c)3 μm and (d)10 μm , respectively .

The self-imaging effect of a single optical micrograting is investigated by a finite-difference time-domain (FDTD) method. The material of the grating is set to be aluminum. Using a 3 μm -period optical micrograting, self-imaging patterns have been obtained as wavelength of the input light ranging from 375nm to 2.2 μm (as shown in Figure 1). In addition, the influence of d has also been analyzed. Irradiated by 635nm-wavelength laser, self-imaging patterns disappear as d going down to 400 nm(as shown in Figure 2). The results indicate that, the self-imaging patterns are more likely observed as d is comparable to λ [9].

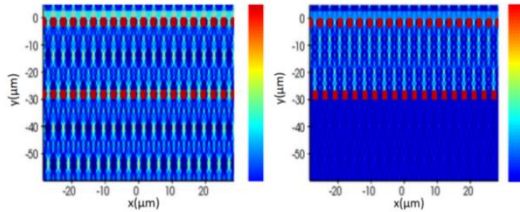


Fig.3. Principle of displacement measurement based on double-grating structure. The simulation diagram of the transmitted field with the lower grating at different positions.

The simulation diagram of the transmitted field of the double-grating structure with a different position of G2 along the x direction is shown in Figure 3. In the simulation, G2 is placed at the first self-imaging position of G1. As $\Delta x=0$, the input light can transmit through G2. However, as $\Delta x=1/2d$, the most of the input light is blocked by G2. The results show that, the overall transmittance of the structure varies with a different position of G2. As a result, the relative displacement detection of upper and lower layers of gratings can be realized in principle by detecting the amplitude of the transmitted light.

III. Experimental results and discussion

A. Experimental setup

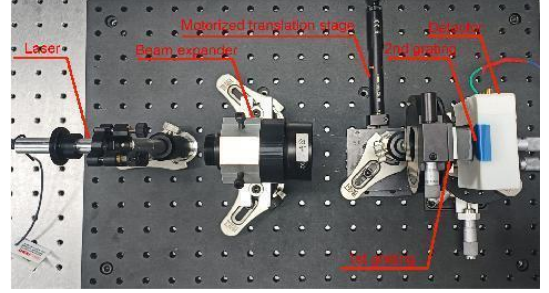


Fig.4. Optical image of the experimental setup

The experimental setup is shown in Figure 4. A laser with a wavelength of 635 nm (model: CPS635R, Thorlabs) is used. The microgratings are prepared by etching aluminum film with a thickness of 150 nm, which is located on a silicon dioxide substrate with a thickness of 500 μm . The periods of G1 and G2 are both 3 μm . The beam incident to the upper grating after passing through a beam expander, leading to self-imaging patterns. G2 is placed behind G1 with a certain distance. By using a multi-quadrant grating and a multi-quadrant detector (OSQ100-IC,OTRON), two sinusoidal signals with a certain phase difference of 90° can be obtained by detecting the amplitude of the transmitted light[8]. After that, the sinusoidal signals are converted into square signals through an interpolation circuit with a subdividing factor of 4096. The displacement can be deduced by calculating the number of square waves.

The resolution (S) of the proposed sensor can be obtained by

$$S = \frac{d}{C} \quad (6)$$

where C is the subdivision factor of the interpolation circuit. In theory, the resolution can be optimized by using grating with smaller period or subdivision circuit with larger multiple.

B. Displacement measurement

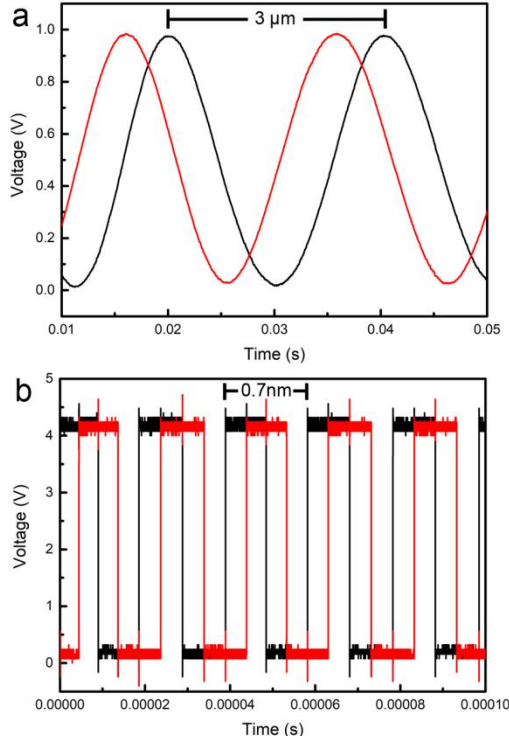


Fig.5. (a)Two sinusoidal curves represent two signals respectively, which obtained by a multi-quadrant detector. The signal period is equal to the grating period. (b)Square signals obtained by combining an interpolation circuit with a subdivision factor of 4096. Resolution is calculated to be $\sim 0.7\text{nm}$.

The sinusoidal signals obtained from the multi-quadrant detector are shown in Figure 5(a). A period of $3\mu\text{m}$ and a phase difference of about 90° is obtained. The period of the sinusoidal signal is equal to that of the gratings, which agrees with Eq. (4). The square signals from the interpolation circuit are shown in Figure 5(b). A resolution of $3\mu\text{m}/4096 \approx 0.73\text{nm}$ is obtained from Eq.(5).

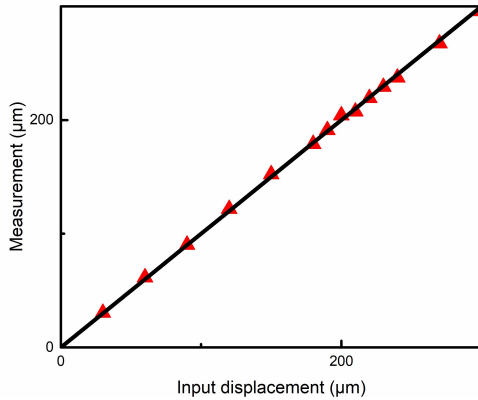


Fig.6. Displacement measurement results within $300\mu\text{m}$. The red triangle symbols represent the results obtained from the proposed sensor. The black line indicates the input displacement.

The the experimental measurement results of the proposed sensor within $300\mu\text{m}$ are shown in Figure 6. A motorized translation stage (MT1/M-Z8, Thorlabs) is used to provide an input displacement. The results show that, the measured results are in good agreement with the input values. The error is measured to be within $5\mu\text{m}$, which may explained by the environment disturbance.

C. Vibration measurement

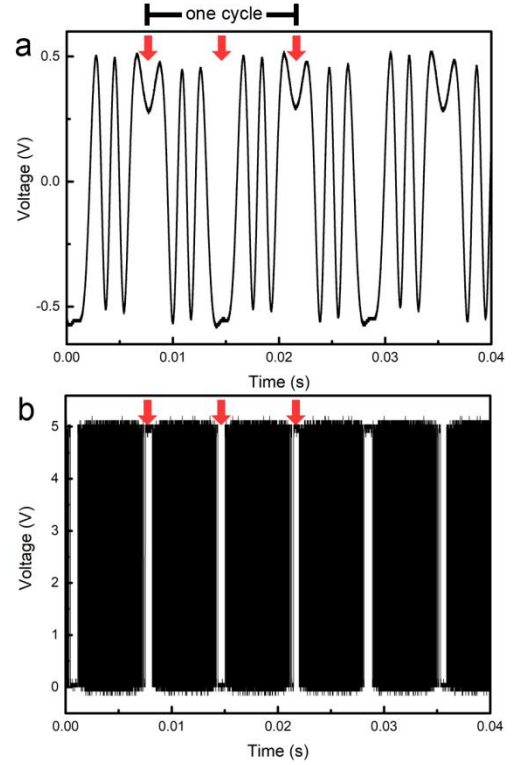


Fig.7. (a)Sinusoidal signal and (b)square signal with a vibration frequency at 70Hz. The red arrows indicate the changing points caused by vibration. The black mark at the top of the figure indicates one single vibration cycle.

The vibration measurement is also demonstrated with the sensor. A piezoelectricceramic is used to offer a vibration. For example, sinusoidal signals and square signals with an input vibration of 70 Hz are shown in Figure 7. Due to the change in the moving direction during the vibration process, periodically changing points are observed. The input vibration frequency can be obtained by calculating the changing points. In this case, the time of one vibration cycle is measured to be $\sim 0.0143\text{s}$. As a result, the vibration frequency is calculated to be 70Hz, which is consistent with the input frequency.

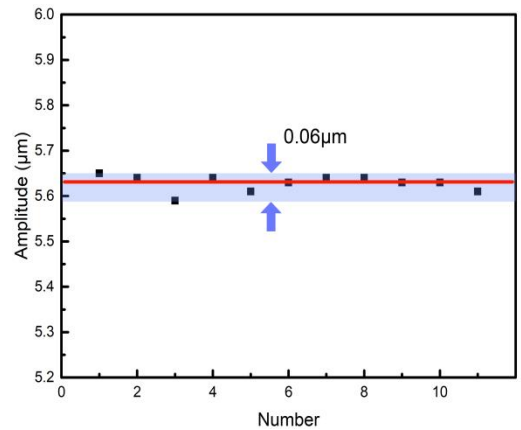


Fig.8. Measurement results of vibration amplitude. The red line represents the input amplitude. The black dots indicate the result of multiple measurements by the sensor. The light-blue area represent the error range.

The amplitude of the vibration can also be measured meanwhile by counting the square signals between two adjacent change points. By changing the pumping voltage of the piezoelectric ceramic, the input amplitude is set to be $\sim 5.5\mu\text{m}$. The amplitude is measured repeatedly for 11 times (as shown in Figure 8), indicating an average of $\sim 5.63\mu\text{m}$ with an error within $0.06\mu\text{m}$. Considering the influence of environmental disturbance, the results show a good repeatability.

IV. Conclusion

Based on the self-imaging effect of optical microgratings, we have demonstrated an ultra-compact sensor for displacement and vibration measurement with resolution down to sub-nanometer level. This experiment provides a new technical path for the development of high-precision displacement sensor.

A double-grating structure is proposed and analyzed by a plane wave interference theory. Using FDTD method, the transmitted field is investigated. The results indicate that, the transmitted amplitude varies as the relative position between the two gratings changing in x direction. By using a multi-quadrant grating and detector, two sinusoidal signals with a phase difference of 90° are obtained within a range of $300\mu\text{m}$ experimentally. Combined with an interpolation circuit with subdivision factor of 4096, 0.73-nm resolution is demonstrated. The experimental results show an error of $5\mu\text{m}$, which may cause from the environment disturbance. The vibration measurement has also been demonstrated in experiment with a frequency of 70Hz . Using a simple

common-path structure, the sensor shows ultra-high compactness without using much optical components, which shows great potential in applications such as precision machining and semiconductor manufacturing.

References

- [1] A Pirati, JV Schoot, K Troost, RV Ballegoij, P Krabbendam, J Stoeldraijer, E Loopstra, J Benschop, J Finders, H Meiling, "The future of EUV lithography: enabling Moore's Law in the next decade," [J]. *Advanced Lithography*, 2017, 10143:101430G.
- [2] N. Anandan and B. George, "A wide-range capacitive sensor for linear and angular displacement measurement," *IEEE Trans. Ind. Electron.* 64(7), 5728–5737 (2017).
- [3] D. Shin and B. Kim, "A laser interferometer encoder with two micromachined gratings generating phase-shifted quadrature," *J. Micromech. Microeng.* 21(8), 085036 (2011).
- [4] W. Lee, N. A. Hall, and F. L. Degertekin, "A grating-assisted resonant-cavity-enhanced optical displacement detection method for micromachined sensors," *Appl. Phys. Lett.* 85(15), 3032–3034 (2004).
- [5] Y. Yin, L. Liu, Y. Bai, J. Irigalantu, H. Yu, Bayanheshig, Z. Liu, W. Li, "Littrow 3D measurement based on 2D grating dual-channel equal-optical path interference," *Opt. express*, 30(23), 41671–41684 (2022).
- [6] Z. Zhang, B. Lei, G. Zhao, Y. Ban, Z. Da, Y. Wang, G. Ye, J. Chen, and H. Liu, "Distance and depth modulation of Talbot imaging via specified design of the grating structure," *Opt. Express* 30(7), 10239–10250 (2022).
- [7] Z. Yang, X. Ma, D. Yu, B. Cao, Q. Niu, M. Li, C. Xin, "An Ultracompact Angular Displacement Sensor Based on the Talbot Effect of Optical Microgratings," *Sensors* 23, 1091 (2023).
- [8] C. Xin, Z. Yang, J. Qi, Q. Niu, X. Ma, C. Fan, M. Li, "Ultra-compact Displacement and Vibration Sensor with A Sub-nanometric Resolution Based on Talbot Effect of Optical Microgratings," *Opt. Express* 30, 40009 (2022).
- [9] J. Wen, Y. Zhang, and M. Xiao, "The Talbot effect: recent advances in classical optics, nonlinear optics, and quantum optics," *Appl. Opt.* 5(1), 83–130 (2013).